Journal of Sound and Vibration (1992) **155**(2), 231–247

FREE VIBRATION ANALYSIS OF A CYLINDRICAL SHELL—CIRCULAR PLATE SYSTEM WITH GENERAL COUPLING AND VARIOUS BOUNDARY CONDITIONS

L. CHENG† AND J. NICOLAS

G.A.U.S., Department of Mechanical Engineering, Université de Sherbrooke, Québec, Canada J1K 2R1

(*Received* 9 *July* 1990 *and in final form* 18 *March* 1991)

The free vibration of a structure consisting of a finite circular cylindrical shell closed at one end by a circular plate is analyzed in this paper. Emphasis is given to the characterization of structural coupling and boundary conditions. These are incorporated into the model by means of continuous distributions of springs along the shell and the plate interface. A general formulation based on a variational principle is used. This formulation allows a wide spectrum of boundary conditions and coupling conditions between the shell and the plate, an issue the importance of which is clearly shown by a literature review. Very good accuracy of the method is demonstrated by solving test problems for lower order modes of the plate and of the shell, for which some results are available in the literature. Comparisons are also made using finite element analysis on a plate-ended shell, showing that the proposed approach is a convenient, efficient and accurate one for determining the modal behavior of such a complex structural system. Other numerical results are then presented for a shell rigidly attached to a plate, to illustrate the coupling phenomena between the shell and the plate. It is shown that there exist three different types of modes for this combined structure; they are termed plate-controlled modes, shell-controlled modes and strongly coupled modes, respectively. It is also shown that each type is closely related to the modal character of each of uncoupled elements.

1. INTRODUCTION

The vibroacoustic study of plates and thin-walled shells have separately received a great deal of attention. When the two structures are coupled together, by allowing energy flow between them, the behavior of the resulting structure is more complex and, consequently, there is less literature available on the topic. However, the study of these combined structures is of great importance in many engineering applications, such as in the design of aeronautical or space structures and industrial vessels. This paper investigates the free vibration characteristics of one variant of these structures: a cylindrical shell coupled to a circular plate at one end, a model which is useful in the case of an aircraft fuselage closed at its end by a circular bulkhead.

The main issue treated in this paper is to establish a general formulation which permits the vibrational analysis of the structure and, in the meantime, allows an extension to vibroacoustic analysis. It can be therefore regarded as a preliminary step which will lead to a final model in which the structure-induced sound field is also considered. A key feature of this investigation is the treatment of elastic boundary conditions and structural coupling. These are incorporated into the model by means of translational and rotational springs

† Currently at Université Laval, Département de Génie Mécanique, Québec, Canada G1K 7P4.

0022–460X/92/110231+17 $03.00/0

along the shell and plate edges and their interface. It is shown in this paper that a variational formulation offers a rather powerful method of simulating such combined structures. As a special case, the circular plate and the cylindrical shell can be treated separately. The extremalization of Hamilton's function is achieved by using the Rayleigh–Ritz method, with simple polynomials and normal modes of a "shear diaphragm supported" shell as admissible functions for the plate and shell, respectively. Natural frequencies and mode shapes can be then calculated numerically.

The modeling of the boundary conditions of the structures, as well as the structural coupling conditions, has always been a substantial difficulty in the vibration and vibro-acoustics analyses of structures. Limited by the methods adopted, classical and idealized boundary conditions are usually chosen. However, in practice the boundary conditions may not always be classical in nature. This may become one of the main sources of discrepancy when the comparison between theory and experiment is made. A recent study [1] has shown that this is particularly true when the structure is coupled to an acoustic enclosure, in which case inaccurate estimations of the boundary conditions affect the nature of the coupling between the structure and the cavity considerably. More realistic models are needed that will be capable of representing the complexities of structural boundary conditions encountered in engineering practice. In recent years, many efforts have been made in this direction with relatively simple structures such as plates and cylindrical shells. In what follows, a literature review focusing on the plate, the shell and the plate-ended shell system is given to support the necessity of the present analysis.

As far as elastic plates are concerned, a large body of literature exists which deals with elastically restrained edges. Numerous investigations have been reported for rectangular plates [2–5] and circular plates [6, 7]. Very good summaries on the subject have been given by Leissa [8] and by Kim and Dickinson [9]. These references have led to a substantial understanding of the effects of boundary conditions on the natural vibrations of plates. However, this paper does not attempt to claim any contribution to the prevailing understanding. Instead, its novelty is in the proposed approach: a variational formulation applied to circular plates with general boundary conditions which encompass all of the boundary conditions previously handled by separate formulations.

For circular cylindrical shells, earlier works [10, 11] have clarified the effects of the classical boundary conditions and their combinations (simply supported, clamped or free edge) on the natural frequencies, as mentioned by Koga in a survey paper [12]. Also, to answer the practical need for simplicity in engineering mechanics, several formulas are available, such as that given by Soedel [13], for natural modes that are dominated by transverse deflection components. In the literature reviewed, and contrary to that for plates, no case of circular cylindrical shells with elastic edge support was found. It is therefore felt that the present analysis, which includes the elastic edge supports, extends the modeling to more realistic boundary conditions.

As to combined shell–plate structures, less literature is available. Recently, for example, some work has been reported by Tavakoli and Singh [14] for a hermetic can which is composed of a circular cylindrical shell with two circular end plates. The authors described a state space method which is, in fact, a transfer matrix based substructuring technique. In that study, a "pinhole" with free edges is introduced at the center of the end plates as the starting point of the analysis, and no special attention is paid to the boundary conditions of the structure. Moreover, an elastic shell–plate attachment is not permitted. It should be further noted that this method, as well as the other commonly used methods for joined structures, such as the receptance method [7] and the transfer matrix method [15, 16], is restricted to free vibration analysis: it soon becomes cumbersome when one wants to deal with the radiation problems of the structure, where the structure is coupled to the acoustic

medium. Consequently, for combined structures, the method described in this paper is believed to include several novelties: first, it models a plate-ended shell structure about which little is known in the literature; second, the structural joint can take any stiffness value; finally, it will easily allow further coupling with the acoustic medium. Consequently, this new model will provide a physical insight into the coupling behavior of the combined structure and provide helpful information to designers.

The organization of this paper is as follows. In section 2, the analytical model and the formulation are stated. Then numerical results are presented and discussed in section 3. First, the case of a single plate or a single shell is considered, showing the flexibility of the model. Wherever possible, comparisons are made with existing values in literature and very good agreement is shown to exist. Then, several results are presented and discussed for a shell rigidly connected to an end plate, illustrating the coupling effects between these two subsystems.

2. ANALYTICAL FORMULATION

2.1. DESCRIPTION OF THE MODEL

The co-ordinate system and various diagrams illustrating the parameters used in the model are shown in Figure 1. The structure consists of a finite circular cylindrical shell with a circular plate at the left end ($x=0$). The shell has a length L and is assumed to be thin; that is, its wall thickness h is much smaller than its radius a. Therefore, the conventional assumptions of Flügge's shell equation are adopted [17]. The shell movement is represented by u, v and w, which are, respectively, the displacements in the longitudinal, tangential and radial directions. The shell is assumed to be initially supported by shear diaphragms at each end, so that the v and w components are restrained at the boundary.

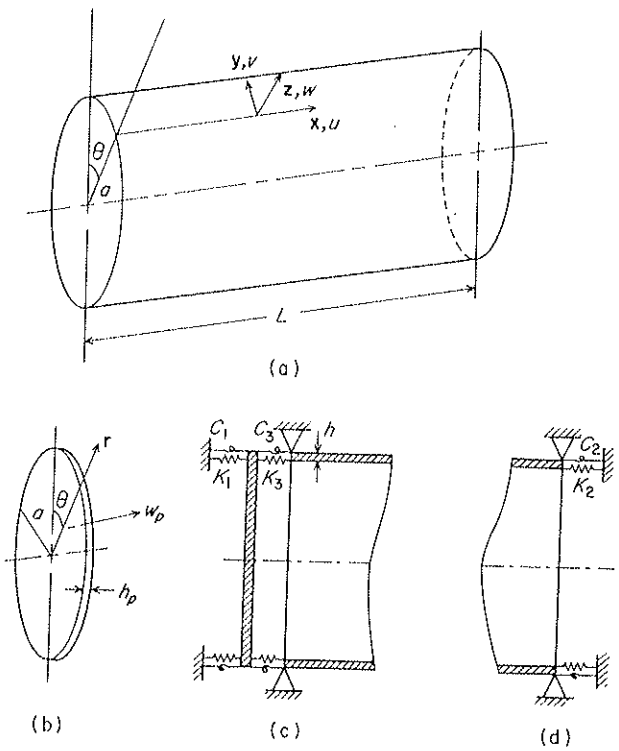

Figure 1. Schematic diagram of the structure and co-ordinate system: (a) cylindrical shell; (b) circular plate; (c) shell-plate interface at $x=0$; (d) elastic support of shell at $x=L$.

The plate–shell joint and the support at $x=L$ can be seen in Figures 1(c) and 1(d) respectively. For the plate, only the normal displacement w_p is taken into account, and it is assumed to be positive along the positive x-axis. The plate has a thickness h_p and is elastically supported by translational and rotational springs having, respectively, distributed stiffnesses K_1 (N/m^2) and C_1 (Nm/m) along its edge. Similar spring systems are introduced between the plate and the shell (K_3, C_3) and at the right end of the shell (K_2, C_2). All of the spring constants are defined in the appropriate units of stiffness per unit length on the contour and are assumed to be constant along the edges.

2.2. VARIATIONAL FORMULATION

The problem under study will now be formulated according to a variational approach. In boundary value problems, one can determine a functional the extremalization of which leads to a solution that is easier to obtain than by solving the actual boundary value problem directly [18]. The reason for this is that the extremalization of the functional can be achieved after expanding the solution over a set of suitable trial functions. By doing this, the method can provide a great degree of flexibility for complex structures.

2.2.1. *Hamilton's principle for the structure*

Hamilton's principle of dynamics states that the displacement of a system adjusts itself in shape and velocity so that Hamilton's function H is minimized. This can be expressed as

$$\delta H = 0. \tag{1}$$

Hamilton's function H is an integral over time of the difference between the kinetic energy and the potential energy of the system, from some initial time t_0 to a specified final time t_1. In the present case, it can be expressed as

$$H = \int_{t_0}^{t_1} (T_c - E_c + T_p - E_p - E_k)\, \mathrm{d}t, \tag{2}$$

where T_c and T_p are, respectively, the kinetic energies of the cylindrical shell and the plate, E_c and E_p are their potential energies, and E_k represents the potential energy stored in the springs. These terms are

$$T_c = \tfrac{1}{2}\rho h \iint \left[\left(\frac{\partial u}{\partial t}\right)^2 + \left(\frac{\partial v}{\partial t}\right)^2 + \left(\frac{\partial w}{\partial t}\right)^2\right] a\, \mathrm{d}\theta\, \mathrm{d}x, \tag{3}$$

$$\begin{aligned} E_c = \frac{Eh}{2(1-\nu^2)} \iint \Bigg[& \left(\frac{\partial u}{\partial x} + \frac{1}{a}\frac{\partial v}{\partial \theta} + \frac{w}{a}\right)^2 + \tfrac{1}{2}(1-\nu)\left(\frac{1}{a}\frac{\partial u}{\partial \theta} + \frac{\partial v}{\partial x}\right)^2 \\ & - 2(1-\nu)\frac{\partial u}{\partial x}\left(\frac{1}{a}\frac{\partial v}{\partial \theta} + \frac{w}{a}\right)\Bigg] a\, \mathrm{d}\theta\, \mathrm{d}x + \frac{Eh^3}{24(1-\nu^2)} \iint \Bigg[\left(\frac{\partial^2 w}{\partial x^2} + \frac{1}{a^2}\frac{\partial^2 w}{\partial \theta^2}\right)^2 \\ & + 2(1-\nu)\left(\frac{1}{a^2}\frac{\partial^2 w^2}{\partial \theta\, \partial x} - \frac{1}{a^2}\frac{\partial^2 w}{\partial x^2}\frac{\partial^2 w}{\partial \theta^2}\right)\Bigg] a\, \mathrm{d}\theta\, \mathrm{d}x, \end{aligned} \tag{4}$$

$$T_p = \tfrac{1}{2}\rho_p h_p \iint \left(\frac{\partial w_p}{\partial t}\right)^2 r\, \mathrm{d}\theta\, \mathrm{d}r, \tag{5}$$

$$E_p=\frac{D_p}{2}\iint\left\{\left(\frac{\partial^2 w_p}{\partial r^2}+\frac{1}{r}\frac{\partial w_p}{\partial r}+\frac{1}{r^2}\frac{\partial^2 w_p}{\partial\theta^2}\right)^2-2(1-\nu_p)\left[\frac{\partial^2 w_p}{\partial r^2}\left(\frac{1}{r}\frac{\partial w_p}{\partial r}\right.\right.\right.$$
$$\left.\left.\left.+\frac{1}{r^2}\frac{\partial^2 w_p}{\partial\theta^2}\right)\right]+2(1-\nu_p)\left[\frac{\partial}{\partial r}\left(\frac{1}{r}\frac{\partial w_p}{\partial\theta}\right)\right]^2\right\} r\,\mathrm{d}\theta\,\mathrm{d}r, \tag{6}$$

$$E_k=\frac{1}{2}\int\left\{\left[K_1 w_p^2+C_1\left(\frac{\partial w_p}{\partial r}\right)^2\right]_{r=a}+\left[K_2 u^2+C_2\left(\frac{\partial w}{\partial x}\right)^2\right]_{x=L}\right.$$
$$\left.+\left[K_3(w_p-u)^2+C_3\left(\frac{\partial w_p}{\partial r}+\frac{\partial w}{\partial x}\right)^2\right]_{x=0}\right\} a\,\mathrm{d}\theta, \tag{7}$$

where ρ, ν and E are, respectively, the density, Poisson ratio, and Young's modulus of the shell material. The same symbols, with the subscript "p" added, are used to denote the equivalent characteristics of the plate material. Finally, $D_p=E_p h_p^3/12(1-\nu_p^2)$ represents the flexural rigidity of the plate.

2.2.2. *Eigenvalue equations of the structure using the Rayleigh–Ritz method*

The essence of the method consists of assuming the solution in the form of a series of admissible functions. In this way, one approximates a system with an infinite number of degrees of freedom by a finite number of degrees of freedom. The admissible functions are required to be linearly independent, regular enough to be differentiable and to satisfy the geometric boundary conditions (related to displacement and slope).

An appropriate choice of the admissible functions in the Rayleigh–Ritz method is a crucial factor on which the accuracy of the prediction depends. This is not an easy task, especially when the structure is complex and when different movements are involved. The difficulty is also increased by the fact that unsuitable choices may make numerical treatment very lengthy and complex. An appropriately established model may certainly facilitate the task. As will be illustrated in the following analysis, the use of distributed springs lessens the need to satisfy the geometric boundary conditions that are required by other possible modeling algorithms. (As one example of these possible approaches, we can consider the work of Bhat [5], where different types of boundary conditions of plates demand different admissible functions.) Our model permits the use of the same admissible functions, to cover a variety of structural coupling and boundary condition cases.

(a) *Admissible functions for the cylindrical shell.* As is pointed out in reference [18], it is possible in many cases to base the decision as to the choice of admissible functions on the knowledge of the eigenfunctions of a slightly different configuration. For cylindrical shell configurations, only the eigenfunctions of a "shear diaphragm supported" shell are available in closed form. This is a shell with its edges fixed in both radial and tangential directions ($w=v=0$) and for which no bending moment and longitudinal membrane force are generated at the boundaries. The terminology "shear diaphragm" has been used by Leissa [17] to distinguish this from another set of edge conditions, where all three displacements (u, v, w), as well as bending moments, are assumed to be zero. The latter case will be referred to as "simply supported" in what follows. The eigenfunctions of the "shear diaphragm supported" shell are used as admissible functions and the expansion of the displacement components is expressed by

$$\begin{Bmatrix}u\\v\\w\end{Bmatrix}=\sum_{\alpha=0}^{1}\sum_{n=0}^{\infty}\sum_{m=1}^{\infty}\sum_{j=1}^{3}A_{nmj}^{\alpha}(t)\begin{Bmatrix}D_{nmj}\sin(n\theta+\alpha\pi/2)\cos(m\pi x/L)\\E_{nmj}\cos(n\theta+\alpha\pi/2)\sin(m\pi x/L)\\\sin(n\theta+\alpha\pi/2)\sin(m\pi x/L)\end{Bmatrix}, \tag{8}$$

where $(D_{nmj}, E_{nmj}, 1)$ are the components of the eigenvector; n and m are the circumferential and longitudinal order; α denotes symmetric ($\alpha = 1$) or antisymmetric ($\alpha = 0$) modes, and j denotes the type of mode (bending, twisting or extension–compression). As can be seen from expression (8), this expansion imposes the condition that v and w be zero at both ends of the shell. Therefore, the only complicating effects that can be added to a model based on the eigenfunctions of a "shear diaphragm supported" shell are those related to the slope (rotation on x-axis) and the longitudinal movement at the boundaries.

(b) *Admissible functions for the plate.* For the plate, any possible deflection or rotation along the edge should be permitted. As a result, no geometric conditions should be imposed *a priori*. A simple polynomial series seems to fit this requirement in the radial direction of the plate. Polynomials have been successfully used for the study of free vibration of beams [19, 20], plates [5], and more recently for the study of sound radiation from rectangular plates [21]. For the circular plate considered here, the polynomial decomposition of the solution is in the form

$$w_p = \sum_{\alpha_p=0}^{1} \sum_{n_p=0}^{\infty} \sum_{m_p=0}^{\infty} B^{\alpha_p}_{n_p m_p}(t) \sin(n_p\theta + \alpha_p\pi/2)(r/a)^{m_p}, \tag{9}$$

where the subscript "p" is added to indicate plate parameters; n_p, m_p and α_p are, respectively, the circumferential order, the radial order and the symmetry index.

(c) *Eigenvalue equations.* For free vibration, it is assumed that

$$A^{\alpha}_{nmj}(t) = A^{\alpha}_{nmj} \sin(\omega t), \qquad B^{\alpha_p}_{n_p m_p}(t) = B^{\alpha_p}_{n_p m_p} \sin(\omega t), \tag{10, 11}$$

where ω is the angular frequency, and A^{α}_{nmj} and $B^{\alpha_p}_{n_p m_p}$ are related to the motion of the shell and the plate.

By substituting equations (8)–(11) into expressions (2)–(7) and minimizing with respect to the unknowns A^{α}_{nmj} and $B^{\alpha_p}_{n_p m_p}$ according to the Rayleigh–Ritz procedure, one finds the eigenvalue equations

$$M_{nmj}(\omega^2_{nmj} - \omega^2)A^{\alpha}_{nmj} + \sum_{m'=1}^{\infty} \sum_{j'=1}^{3} X^{\alpha}_{nmjm'j'} A^{\alpha}_{nm'j'} - \sum_{m_p=0}^{\infty} Y^{\alpha}_{nmjm_p} B^{\alpha}_{nm_p} = 0, \tag{12}$$

$$\sum_{m_p'=0}^{\infty} (R^{\alpha}_{nm_pm_p'} - \omega^2 M^{\alpha}_{nm_pm_p'}) B^{\alpha}_{nm_p'} + \sum_{m_p'=0}^{\infty} Z^{\alpha}_{nm_pm_p'} B^{\alpha}_{nm_p'} - \sum_{m=1}^{\infty} \sum_{j=1}^{3} Y^{\alpha}_{nmjm_p} A^{\alpha}_{nmj} = 0, \tag{13}$$

where

$$X^{\alpha}_{nmjm'j'} = aN^{(1)}_{\alpha n}[D_{nmj} D_{nm'j'}(K_3 + \Delta_m\Delta_{m'} K_2) + (m\pi/L)(m'\pi/L)(C_3 + \Delta_m\Delta_{m'} C_2)],$$

$$Y^{\alpha}_{nmjm_p} = aN^{(1)}_{\alpha n}[D_{nmj} K_3 - (m\pi/L)(m_p/a)C_3],$$

$$Z^{\alpha}_{nm_pm_p'} = aN^{(1)}_{\alpha n}[K_1 + K_3 + (m_p/a)(m_p'/a)(C_1 + C_3)], \tag{14}$$

$$N^{(1)}_{\alpha n} = \begin{cases} \pi, & \text{for } n \neq 0 \\ 0, & \text{for } n = 0 \text{ and } \alpha = 0 \\ 2\pi, & \text{for } n = 0 \text{ and } \alpha = 1 \end{cases}, \qquad \Delta_m = \begin{cases} 1, & \text{for } m \text{ odd} \\ -1, & \text{for } m \text{ even} \end{cases},$$

and where $n = 0, 1, 2, \ldots$; $m_p, m_p' = 0, 1, 2, \ldots$; $m, m' = 1, 2, 3, \ldots$; $j, j' = 1, 2, 3$; and $\alpha = 0, 1$. In the above expressions, ω_{nmj} and M_{nmj} are, respectively, the natural frequencies and the generalized masses of the "shear diaphragm supported" shell, two quantities that can be easily calculated. m_p', m' and j' have the same meaning as m_p, m and j. $R^{\alpha}_{nm_pm_p'}$, and

$M^{\alpha}_{nm_pm_p'}$, the stiffness and mass terms of the plate, are given by

$$R^{\alpha}_{nm_pm_p'} = (D_p \Psi_{m_pm_p'}/a^2)\{N^{(1)}_{\alpha n}[(m_p^2-n^2)(m_p'^2-n^2)-(1-\nu_p)m_p(m_p-1)(m_p'-n^2) - (1-\nu_p)m_p'(m_p'-1)(m_p^2-n^2)]+2(1-\nu_p)N^{(2)}_{\alpha n}n^2(m_p-1)(m_p'-1)\}, \quad (15)$$

$$M^{\alpha}_{nm_pm_p'} = a^2\rho_p h_p N^{(1)}_{\alpha n}/(m_p+m_p'+2), \quad (16)$$

where

$$\Psi_{m_pm_p'} = \begin{cases} 0, & \text{for } m_p+m_p'-2 \leqslant 0, \\ 1/(m_p+m_p'-2), & \text{otherwise,} \end{cases}$$

$$N^{(2)}_{\alpha n} = \begin{cases} \pi, & \text{for } n \neq 0, \\ 0, & \text{for } n=0 \text{ and } \alpha=1, \\ 2\pi, & \text{for } n=0 \text{ and } \alpha=0. \end{cases} \quad (17)$$

An examination of equations (12) and (13) shows that the shell and the plate are coupled to each other via the last term on the left side, which is a function of the elastic constants K_3 and C_3. However, due to the axial symmetry of the structure, the movements with different circumferential order n or symmetry index α are uncoupled. This enables one to solve equations (12) and (13) for every given n and α. Naturally, this property relies on the axial symmetry of the structure, and is no longer true if non-axisymmetrical elements are included. The solution yields the natural frequencies, together with the coefficients for mode shapes.

3. NUMERICAL RESULTS AND DISCUSSION

Using the analytical approach formulated above, numerical results are presented for several specific cases to illustrate its utility. The objective is twofold: (1) to compare the present results with previously published ones to validate the method, and (2) to give supplementary results with respect to the literature, especially when the plate is coupled to the shell.

Beforehand, several remarks should be made. First, it is known that an elastically restrained edge has boundary conditions which are intermediate between appropriate classical boundary conditions. The latter can be obtained as special cases by simply setting the appropriate constants K_i or C_i ($i=1, 2, 3$) equal to either zero or infinity. For infinity, one in fact takes a large enough quantity in the calculations. Second, for each calculation, the number of terms used in the series (expressions (8) and (9)) is increased until a relatively stable solution is achieved. It has been observed during numerical calculations that the solution converges rather rapidly and the number of terms retained in the numerical expansions is given for each case. Another specification, related to the choice of the polynomial series (9) for a plate, is worth noting. The final plate mass matrix, the elements of which are calculated by expression (16), is actually a Hilbert matrix. Mathematically, this matrix is ill-conditioned when its size becomes large and, therefore, special care is needed to control the certainty of the computations. This property limits the number of polynomial terms retained in the series. As a result, the evaluations of some higher order modes of the plate (those with a large radial wavenumber) may be difficult. This difficulty may be overcome when one deals with the forced response of the structure, since the stiffness matrix will join the mass matrix to form the system matrix, which may no longer be ill-conditioned. In the present analysis, the eigenvalue equations (12) and (13) are

solved by using the IMSL software (Edition 1.1, 1989), in which the Cholesky factorization is calculated and the accuracy of the solutions is controlled by a performance index. As will be illustrated, the lower order modes of the plate can be estimated quite accurately.

3.1. COMPARISON WITH AVAILABLE RESULTS FOR THE NATURAL FREQUENCIES OF A CIRCULAR PLATE WITH ELASTIC SUPPORTS

The first case treated is that of a circular plate, elastically supported by translational and rotational springs uniformly distributed around its edge. Complete results for the same problem have been reported by Azimi [7], who used the receptance method. Although all cases treated in his paper have been tested using our approach during the study, only one representative case with elastical support is reported here in Table 1. For the comparison with Azimi's solution (values in parentheses), numerical results for the first three natural frequencies are given for the circumferential order $n=0$, 1, 2. The integer i is used to indicate the number of nodal circles on the plate (not including the edge). For these calculations, 13 terms were used in the polynomial series. It can be seen that the discrepancies between the two solutions are very small. Very good agreement is also noticed with all of the other results given in reference [7]. Among all those cases considered, but not reported here, the worst case found is the mode $n=0$ and $i=2$ for the clamped case, with a discrepancy of 0·15%. In comparison with the receptance method mentioned above, one can see that the present variational analysis provides a general formulation which gives comparable accuracy.

TABLE 1

Values of $\omega_{in}a^2(\rho_p h_p/D_p)^{1/2}$ *for circular plates with elastical supports: results in parentheses are taken from reference* [7]

Boundary conditions	Number of nodal circles, i	$n=0$	$n=1$	$n=2$
$K_1a^3/D_p=10$	0	4·128 (4·127)	6·064 (6·064)	10·182 (10·181)
	1	14·498 (14·498)	26·840 (26·840)	42·217 (42·213)
$C_1a/D_p=10$	2	46·085 (46·085)	68·294 (68·294)	93·444 (93·432)

3.2. COMPARISON WITH AVAILABLE RESULTS FOR THE NATURAL FREQUENCIES OF A SHELL WITH SEVERAL CLASSICAL BOUNDARY CONDITIONS

The second problem considered is that of a finite circular cylindrical shell with several boundary conditions. The shell is made of steel with a radius of 3·0 in (0·0762 m), a length of 12 in (0·3048 m) and a thickness of 0·01 in ($2{\cdot}54\times10^{-3}$ m). The material constants are $E=29{\cdot}6\times10^6$ psi ($2{\cdot}04\times10^{11}$ N/m^2), $\nu=0{\cdot}29$, $\rho=0{\cdot}733\times10^{-3}$ lb-s^2/in^4 (7838·6 kg/m^3). The same configuration has been used by Vronay and Smith [11] to find the exact natural frequencies of the shell. A typical comparison for a clamped shell (C–C) is given in Table 2. In the numerical calculations, 40 terms in the longitudinal direction were considered. Calculated frequencies for the first four radial modes, having one to five circumferential waves, are compared with the results of reference [11] (values in parentheses). The agreement between the two sets of results is very good. Indeed, for most cases, the results agree within 1%. The same observation has been made for other tested cases (four cases have been tested). This comparison, together with the one made for the plate configuration, serves to provide confidence in the validity of the solution.

TABLE 2

Values of natural frequency (Hz) *for a cylindrical shell with clamped boundary conditions* (C–C). *Results in parentheses are taken from reference* [11]

Number of axial nodal circles, P	$n=1$	$n=2$	$n=3$	$n=4$	$n=5$
0	3429 (3423)	1922 (1917)	1163 (1154)	769 (765)	581 (581)
1	6504 (6412)	4062 (3902)	2659 (2536)	1832 (1752)	1335 (1287)
2	8490 (8493)	5845 (5832)	4065 (4051)	2938 (2918)	2210 (2190)
3	9455 (9418)	7307 (7299)	5480 (5442)	4155 (4100)	3222 (3165)

3.3. NATURAL FREQUENCIES OF A SHELL WITH ELASTIC RESTRAINING EFFECTS

The third problem treated is a circular cylindrical shell, "shear diaphragm supported" at the right end ($x=L$), and with elastic restraining at the left end ($x=0$). The shell is elastically restrained against rotation along the left edge by C_3 and the translational spring K_3 is introduced to create axial restraint. As far as we know, this case has not been previously reported in the literature. Let us define a dimensionless factor Ω, which will be referred to as the frequency parameter. It is the ratio between the natural frequency and the ring frequency, the latter being defined as

$$f_r = 1/(2\pi a)\sqrt{E/\rho(1-\nu^2)}. \tag{18}$$

In Table 3 are given the values of Ω for the first three modes of the shell ($L/a=3$ and $a/h=30$) when $n=0$, 1 and 2, respectively. One can see a variety of intermediate cases among several extreme ones: "shear diaphragm supported" ($K_3=C_3=0$), clamped without axial strain ($K_3=0$, $C_3=\infty$), simply supported ($K_3=\infty$, $C_3=0$) and clamped ($K_3=C_3=\infty$). It can be seen from this table that the effect of axial constraint due to K_3 is generally more significant than that of clamping due to C_3, an important conclusion already outlined by Forsberg [10] for the minimum natural frequency. In addition, one can see that this conclusion is true to a greater or lesser degree for almost all modes listed in Table 3. Generally speaking, the lower the natural frequency is, the more it is affected by the axial constraining effect. It is worth noting that all values shown in this table are lower than the ring frequency of the shell [18]. This is a frequency range in which membrane effects are large.

3.4. PLATE-ENDED SHELL: NATURAL FREQUENCIES, MODE SHAPES AND COUPLING ANALYSES

Investigations carried out above demonstrate that the behavior of shells and plates are well characterized by the established model and the chosen admissible functions. This section concentrates on the plate-ended cylindrical shell. The natural frequencies and corresponding mode shapes are presented first. Then emphasis is placed on the analysis of the coupling between the shell and the plate, the intention being not only to give a comprehensive understanding of the phenomena related to the structure in question, but also to offer concepts and guidelines that may be applicable to the analysis of other combined structures. Although the formulation was established to study systems with elastic junctions or elastic supports, the results presented here are restricted to the one specific case of a rigid shell–plate junction because of the limitless combinations which can arise. Another reason for choosing this limiting case is that other cases with elastic junctions can be easily evaluated from the knowledge of this limiting coupled case (infinite stiffness

TABLE 3

Values of frequency parameter Ω of a cylindrical shell elastically supported at $x=0$, shear diaphragm supported conditions at $x=L$, $L/a=3$, $a/h=30$ (p=number of axial nodal circles, not including edge)

		K_3a^3/D											
		0			10^3			10^5			∞ (10^8)		
		p			p			p			p		
C_3a/D	n	0	1	2	0	1	2	0	1	2	0	1	2
0	1	0·3727	0·7127	0·8503	0·3751	0·7127	0·8504	0·3971	0·7128	0·8507	0·3995	0·7128	0·8507
	2	0·1847	0·4643	0·6630	0·1876	0·4648	0·6630	0·2208	0·4712	0·6634	0·2257	0·4723	0·6634
	3	0·1276	0·3169	0·5085	0·1292	0·3176	0·5087	0·1521	0·3305	0·5120	0·1560	0·3334	0·5127
10	1	0·3730	0·7136	0·8521	0·3754	0·7136	0·8521	0·3977	0·7137	0·8523	0·4001	0·7137	0·8523
	2	0·1856	0·4658	0·6654	0·1885	0·4663	0·6655	0·2217	0·4730	0·6659	0·2266	0·4741	0·6660
	3	0·1290	0·3192	0·5118	0·1306	0·3140	0·5120	0·1529	0·3329	0·5156	0·1568	0·3358	0·5164
10^2	1	0·3734	0·7145	0·8535	0·3758	0·7145	0·8536	0·3984	0·7146	0·8537	0·4009	0·7146	0·8537
	2	0·1868	0·4676	0·6680	0·1896	0·4681	0·6681	0·2220	0·4751	0·6687	0·2277	0·4763	0·6688
	3	0·1308	0·3221	0·5157	0·1323	0·3228	0·5159	0·1539	0·3357	0·5197	0·1576	0·3386	0·5206
∞ (10^8)	1	0·3735	0·7147	0·8539	0·3760	0·7148	0·8539	0·3986	0·7149	0·8540	0·4011	0·7149	0·8540
	2	0·1871	0·4681	0·6687	0·1900	0·4686	0·6687	0·2232	0·4757	0·6694	0·2280	0·4769	0·6695
	3	0·1313	0·3229	0·5167	0·1328	0·3236	0·5169	0·1542	0·3365	0·5208	0·1579	0·3394	0·5217

of the springs at the joint) and that of the uncoupled cases (zero stiffness of the springs at the joint).

The shell and plate considered are assumed to have the same thickness and material properties. The geometrical parameters used are $a/h=30$ and $L/a=3$. The shell is "shear diaphragm supported" at the right end ($x=L$) and rigidly connected to the plate at $x=0$ ($K_3=C_3=\infty$). We also assume that $K_1=\infty$ and $C_1=0$. Therefore, the two subsystems (plate and shell) are coupled to each other only through the sloping along the edge. Numerical studies were carried out, during which 11 and 40 terms were taken for the plate and shell, respectively.

In Figure 2 are given the first six mode shapes, together with the values of the frequency parameter Ω for the symmetric modes ($\alpha=1$) having a circumferential order $n=2$. These figures show the normal displacement of the plate (w_p) and the radial displacement of the shell (w) in the cross-section for $\theta=0$ and $\theta=\pi$. As expected, the plate and shell vibrations are usually coupled. However, one can notice some cases where the coupling is rather

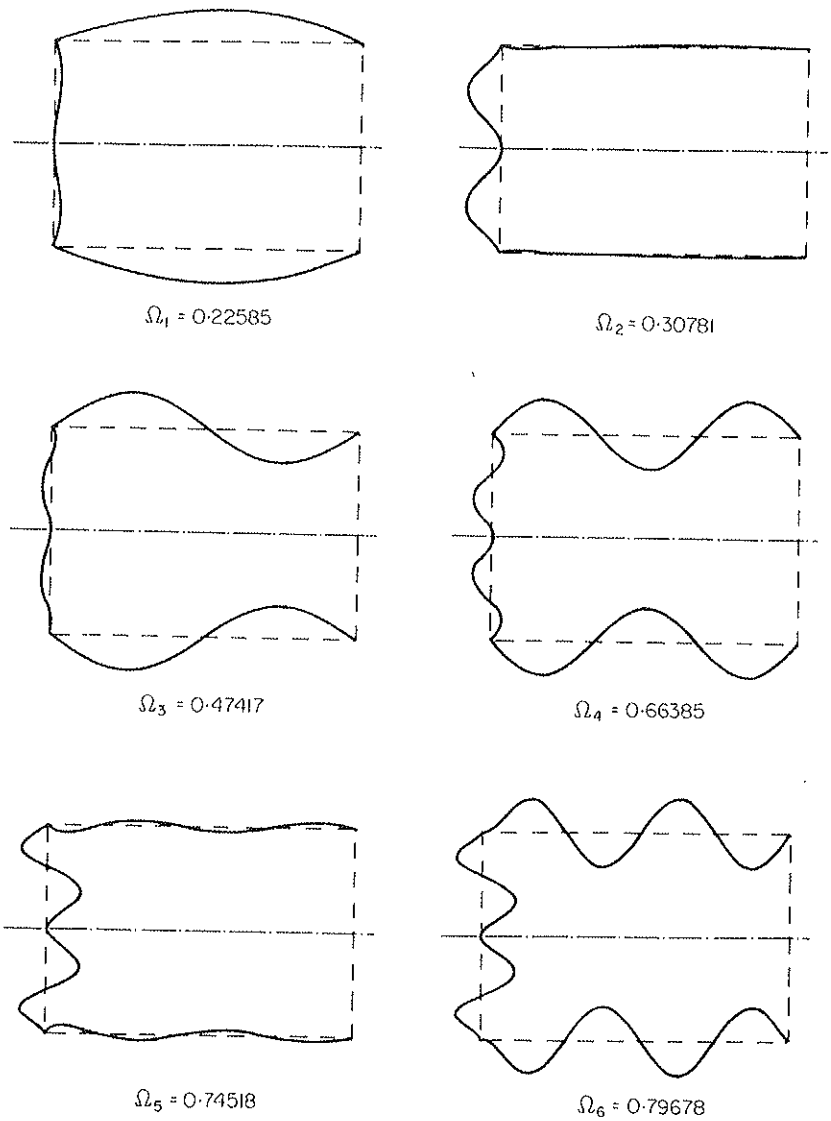

Figure 2. First six mode shapes and frequency parameters Ω of a shell rigidly connected to a plate. The right end of the shell is "shear diaphragm supported" ($n=2$; $\alpha=1$, $a/h=30$, $L/a=3$).

weak. For example, the first mode is dominated by shell vibrations, whereas the second one is essentially a plate mode.

For the same plate-ended shell, our results are compared to those obtained via the finite element method (FEM). The finite element software used is a commercially available one (ANSYS 4.4A). A 19×20 finite element mesh (circumferential and longitudinal directions respectively) is used for the shell and a 20×20 mesh (circumferential and radial directions respectively) for the plate. All calculations are carried out using an IRIS-4D computer. As we are limited by the computational facilities required for finite element analysis, only the first three modes for $n=2$ are obtained. Frequency parameters, together with the calculation time taken by each approach, are tabulated in Table 4. It can be seen that the agreement between both sets of results is excellent. As far as mode shapes are concerned, it has been observed that the two approaches give exactly the same description, and even very detailed deformations around the shell–plate junction are precisely predicted by present analysis. In terms of computation time, however, our approach is much less time-consuming than the finite element analysis. In conclusion, it appears that the present approach is a very convenient, efficient and accurate one for determining the modal behavior of a rather complex structure system.

TABLE 4

Comparison of frequency parameters between the present study and the finite element method for the case of a plate-ended shell ($L/a=3$, $a/h=30$), q = *mode rank*: $\xi = (\textit{present study} - \textit{FEM})/\textit{present study}$

Mode order n, q		Present study	FEM	Deviation, ξ(%)
2	1	0·22585	0·22005	2·5
2	2	0·30781	0·30280	1·6
2	3	0·47417	0·47450	−0.07
CPU time (s)		20.6	5671	

In order to understand the phenomena of coupling, let us consider how the coupling behavior changes with the variation of the geometric parameters of the structure. To this end, the same plate-ended shell system was used to show the variation of the frequency parameter Ω *vs.* the length to radius ratio L/a of the shell. For a given radius, the shell length was gradually increased up to $L/a=4$. This is illustrated in Figure 3, where the first four modes of the structure are shown when $n=2$. To quantify the extent of the coupling, define λ as $10 \log (w_{max}/w_{p\,max})$ for each structure mode, with w_{max} and $w_{p\,max}$ being, respectively, the maximum displacements of the shell and the plate. According to this factor, one knows that the coupling between shell and plate is strong if λ is near zero, which corresponds with the case in which the shell displacement is of the same order of magnitude as that of the plate. For the same configuration the variation of λ is shown in Figure 4, where the four curves correspond to those drawn in Figure 3. A very representative example is the first mode (solid curve C_1 in both diagrams). It can be seen from these two figures that when the shell is short, Ω is almost constant and the deflection of the end plate is dominant ($\lambda < 0$). One can say that in this range the vibrations are plate-controlled. Strong coupling occurs when L/a reaches a value of 2·5, where λ is near zero. Beyond this range, the plate is stiffer than the shell and the vibrations become shell-controlled. In this case, Ω decreases as the shell length increases. These observations also apply to the other modes presented in Figures 3 and 4, for which plate-controlled, shell-controlled and strongly coupled vibrations appear successively as L/a changes.

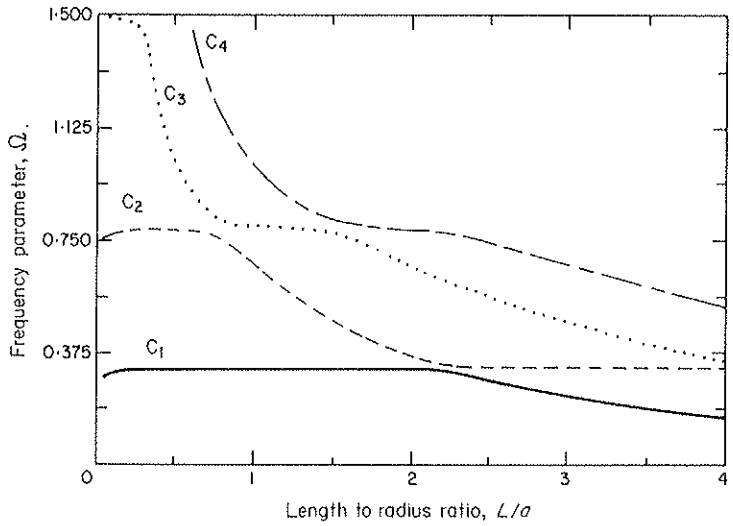

Figure 3. Variation of the frequency parameter Ω *vs.* the length to radius ratio (L/a) for the first four modes of a plate-ended shell. The boundary conditions are the same as in Figure 2.

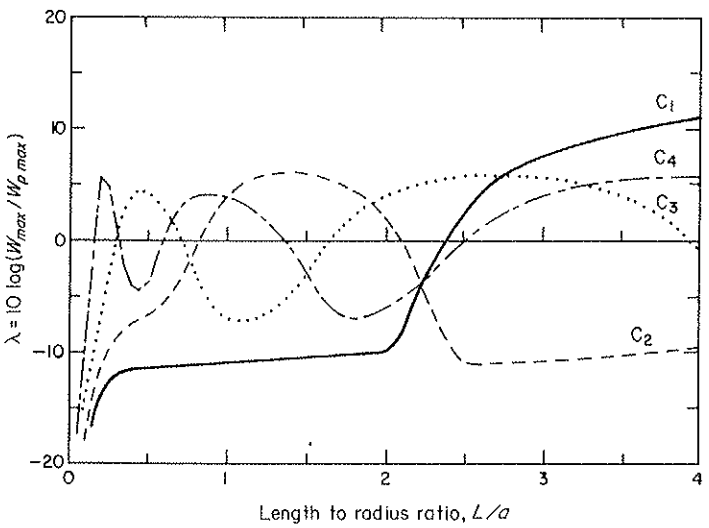

Figure 4. Variation of the maximum displacement ratio between a shell and plate *vs.* the length to radius ratio (L/a). The boundary conditions are the same as in Figure 2.

It is of great interest if one could know, even approximately, the modal behavior of a coupled system from knowledge of the behavior of each component, which is usually easier to obtain. The aim is twofold. When two structures are coupled, what will their natural frequencies be and which component will dominate the corresponding movement? To this end, it is revealing to inspect Figure 5, in which the curve C_1, already shown in Figure 3, which is the first mode of the coupled structure, is drawn together with the first natural frequencies of the shell and the plate when they are uncoupled and with two extreme edge conditions at $x=0$: a clamped case (two dotted lines CP_1 and CS_1 for the plate and shell respectively) and a supported case (two dashed lines SP_1 and SS_1 for the plate and the shell respectively). In all cases, a "shear diaphragm supported" condition is used at the right end of the shell. It can be seen that when the shell is short (corresponding to a small value of L/a), the value of Ω for either the simply supported plate or clamped plate is much lower than that of the shells. Hence the shell is much stiffer than the plate. When

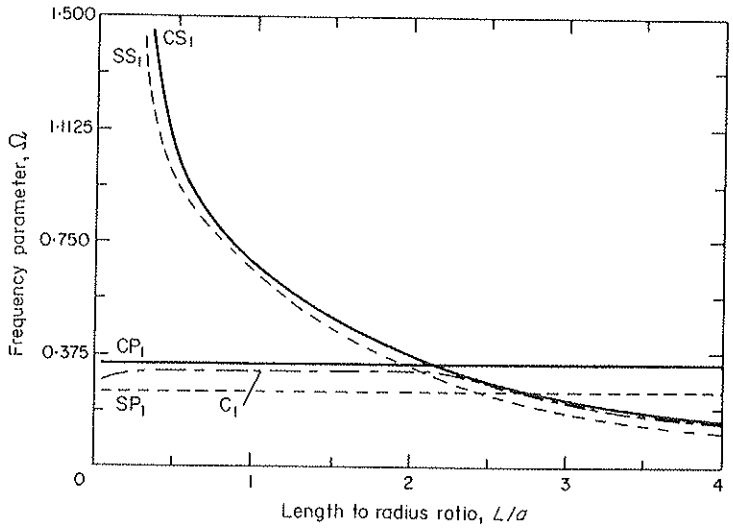

Figure 5. Variation of the frequency parameter Ω *vs.* the length to radius ratio L/a for the first mode of three different structures: plate, shell and plate-ended shell. Boundary conditions of the structures at $x=0$ are as follows: C_1 = plate-ended shell with the same boundary conditions as in Figure 2; SP_1 = simply supported plate; CP_1 = clamped plate; SS_1 = "shear diaphragm supported" shell; CS_1 = clamped shell.

they are combined, one can expect that the first mode of the structure will have a panel-like behavior, indicating that the plate is responsible for the mode. Its natural frequency is lower than that of the clamped panel but higher than that of the simply supported one because of restraining effects due to the shell. When L/a has a value of about 2·5, frequency coincidence occurs between these two uncoupled structures. The combined structure exhibits strong coupling between the plate and the shell. With an increase in shell length, the natural frequencies of the shell alone become lower than that of the plate. Therefore, the natural frequency of the combined structure is close to that of the shell alone with clamped edge conditions. The behavior of the structure is expected to be shell-like, with negligible motion of the plate. In Figure 6 is shown a similar comparison for the first four structure modes, already illustrated in Figure 3. In comparison with the corresponding uncoupled structures, the same conclusion can be drawn, except that several panel-like, coincidence or shell-like ranges are observed for higher order modes. Physically, a coincidence range corresponds to a mechanical impedance adaptation of the uncoupled structures, whereas a panel-like or shell-like range corresponds to a frequency range where the mechanical impedances of the uncoupled components are quite different.

It should be pointed out that this analysis is possible only for the lower frequency modes where the modal density is lower. Also it is more qualitative than quantitative and the accuracy of the estimates of the natural frequencies of the combined structure depends on the character of the mode. Naturally, an accurate quantitative estimate can be given only by numerical evaluation of the coupled system solutions.

4. CONCLUDING REMARKS

Analytical and numerical results have been presented in this paper to study the free vibration problems of circular plates, cylindrical shells and their combination. Special attention has been paid to simulations of a variety of boundary conditions and elastic junctions of the structure. This is done through a spring system along all edges of the structure, and the problem is formulated using a variational approach.

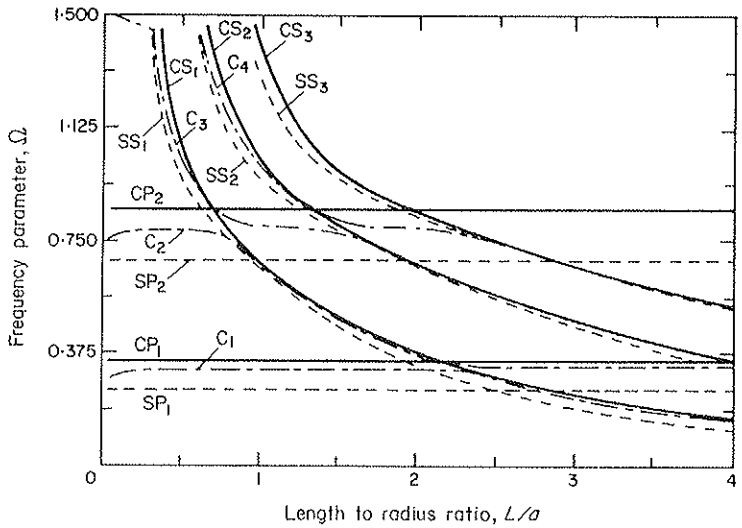

Figure 6. Variation of the frequency parameter Ω *vs.* the length to radius ratio L/a for the modes of three different structures: plate, shell and plate-ended shell. Boundary conditions of the structures at $x=0$ are as follows: C_1, C_2, C_3, C_4 = first four natural modes of a plate-ended shell with the same boundary conditions as in Figure 2; SP_1, SP_2 = first two natural modes of a simply supported plate; CP_1, CP_2 = first two natural modes of a clamped plate; SS_1, SS_2, SS_3 = first three natural modes of a "shear diaphragm supported" shell; CS_1, CS_2, CS_3 = first three natural modes of a clamped shell.

This analysis presents an attempt to make an improvement on work existing in the literature in the following areas: (1) various boundary conditions of the structure are simulated in a general formulation (the structure may be a plate alone, a shell alone or their combination—the boundary conditions may be either classical cases or elastic support cases); (2) different joint conditions between the plate and the shell are permitted—this joint may be rigid or elastic; (3) a coupling analysis provides physical insight into the coupling behavior of the combined structure and gives helpful hints to designers; (4) the formulation can be easily extended to the vibroacoustic problem.

The versatility of the method has been shown through several typical examples. First of all, applications of the method to a few selected cases for plates and shells yielded results that agree well with results obtained from other methods. The case of a cylindrical shell rigidly connected to an end panel was chosen to reveal coupling phenomena between the two substructures. Both coupled and weakly coupled vibrations occur in the structure. More specifically, they can be divided into three groups: plate-controlled modes, shell-controlled modes and strongly coupled modes. A coupling analysis showed the relationships between the coupled structure and the uncoupled substructures in terms of natural frequencies. It gives some guidelines for analyzing the character of the lower order modes of such coupled structures, on the basis of knowledge of the modes of its components, which usually are easier to obtain. This might offer useful information for the design of such combined structures.

Our study has concentrated on some axisymmetric cases. In a more general context, the method applies appropriately to cases in which non-axisymmetric elements are present. These elements may be non-uniformly distributed boundary and joint conditions, local masses or stiffeners. In these cases, contrary to the present study, coupling occurs between the modes of different circumferential order so that numerical treatment of the problem involves matrices of larger size. As to forced vibration problems, the application of the method is straightforward. Only supplementary terms corresponding to the work done by external forces have to be included in Hamilton's function. It seems that the next step in

this investigation should be the study of the dynamic response and the sound radiation into the cavity which is surrounded by the structure. Based on the knowledge of the modal behavior obtained by the present analysis, this further study is expected to give a better understanding of the vibroacoustic behavior of such combined structures.

ACKNOWLEDGMENTS

This work was supported by The Dynamics Group of Canadair whose efficient collaboration is very much appreciated.

The authors are also indebted to J. Allard for providing the finite element analysis results used in this paper.

REFERENCES

1. L. CHENG and C. LESUEUR 1989 *Journal d'Acoustique* **2**, 347–355. Influences des amortissements sur la réponse vibroacoustique. Etude théorique et expérimentale d'une plaque excitée mécaniquement et couplée à une cavité.
2. P. A. A. LAURA and R. GROSSI 1978 *Journal of Sound and Vibration* **59**, 355–368. Transverse vibrations of a rectangular plate elastically restrained against rotation along three edges and free on the fourth edge.
3. P. A. A. LAURA and R. GROSSI 1981 *Journal of Sound and Vibration* **75**, 101–107. Transverse vibrations of rectangular plates with edges elastically restrained against translation and rotation.
4. G. B. WARBURTON and S. L. EDNEY 1984 *Journal of Sound and Vibration* **95**, 537–552. Vibrations of rectangular plates with elastically restrained edges.
5. R. B. BHAT 1985 *Journal of Sound and Vibration* **102**, 493–499. Natural frequencies of rectangular plates using characteristic orthogonal polynomials in Rayleigh–Ritz method.
6. A. W. LEISSA, P. A. A. LAURA and R. H. GUTIERREG 1979 *Journal of the Acoustical Society of America* **66**, 180–184. Transverse vibrations of circular plates having non uniform edge constraints.
7. S. AZIMI 1988 *Journal of Sound and Vibration* **120**, 19–35. Free vibration of circular plates with elastic edge supports using the receptance method.
8. A. W. LEISSA 1987 *The Shock and Vibration Digest* **19**, 11–18. Recent studies in plate vibrations, 1981–1985, part I: classical theory.
9. C. S. KIM and S. M. DICKINSON 1989 *Journal of Sound and Vibration* **134**, 407–421. On the free, transverse vibration of annular and circular, thin, sectorial plates subject to certain complicating effects.
10. K. FORSBERG 1964 *American Institute of Aeronautics and Astronautics Journal* **2**, 2150–2157. Influence of boundary conditions on the modal characteristics of thin cylindrical shells.
11. D. F. VRONAY and B. L. SMITH 1970 *American Institute of Aeronautics and Astronautics Journal* **8**, 601–603. Free vibration of circular cylindrical shells of finite length.
12. T. KOGA 1989 *Journal of the Japan Society of Mechanical Engineers, Serie I*, **32**, 311–319. Free vibrations of circular cylindrical shells.
13. W. SOEDEL 1980 *Journal of Sound and Vibration* **70**, 309–317. A new frequency formula for closed circular cylindrical shells for a variety of boundary conditions.
14. M. S. TAVAKOLI and R. SINGH 1990 *Journal of Sound and Vibration* **136**, 141–145. Modal analysis of a hermetic can.
15. T. IRIE, G. YAMADA and Y. MURAMOTO 1984 *Journal of Sound and Vibration* **95**, 31–39. Free vibration of joined conical-cylindrical shells.
16. T. IRIE, G. YAMADA and Y. MURAMOTO 1984 *Journal of Sound and Vibration* **92**, 107–115. The axisymmetrical response of a circular cylindrical double-shell system with internal damping.
17. A. W. LEISSA 1973 *Vibration of Shells*. NASA SP-288. Washington, D.C.
18. L. MEIROVITCH 1967 *Analytical Methods in Vibrations*. New York: Macmillan.
19. R. B. BHAT 1986 *Journal of Sound and Vibration* **105**, 199–210. Transverse vibrations of a rotating uniform cantilever beam with tip as predicted by using beam characteristic orthogonal polynomials in the Rayleigh–Ritz method.
20. C. S. KIM and S. M. DICKINSON 1988 *Journal of Sound and Vibration* **122**, 441–455. On the analysis of laterally vibrating slender beams subjected to various complicating effects.

21. A. BERRY, J. L. GUYADER and J. NICOLAS 1990 *Journal of the Acoustical Society of America* **88**, 2979–2802. A general formulation for the sound radiation from rectangular, baffled plates with arbitrary boundary conditions.
22. B. LAULAGNET and J. L. GUYADER 1989 *Journal of Sound and Vibration* **131**, 397–415. Modal analysis of a shell's acoustic radiation in light and heavy fluids.